Journal of Applied Sciences

ISSN 1812-5654

Journal of Applied Sciences 9 (14): 2584-2591, 2009
ISSN 1812-5654

Hollow Concrete Poles with Polymeric Composite Reinforcement

N. Taranu, G. Oprisan, M. Budescu and I. Gosav
Faculty of Civil Engineering and Building Services, Iasi, Romania

Abstract: The results of a theoretical and experimental study carried out on the possibility of using polymer composite reinforcing elements for a power supply hollow Reinforced Concrete (RC) column are presented in the study. The composite reinforcing elements are utilized both as longitudinal glass reinforced thermosetting polymer (vinylester) bars and transverse reinforcement made of a Glass Fibre Reinforced Polypropylene (GFPP) spiral. The columns have been fabricated using the existing manufacture facilities based on centrifuge procedure. An experimental program has been organized to evaluate the structural response of spun-cast elements according to existing standard tests. A number of loading cycles of lateral action have been applied on the posts up to failure. Cracks development and the corresponding loading stages have been recorded. A theoretical analysis has been performed to prove the suitability of existing calculation formulas for serviceability and ultimate limit states. This study confirms the possibility of using composite reinforcement for hollow tapered RC columns.

Key words: Tapered columns, composite materials, hybrid structures, concrete-reinforcement bonding, structural response

INTRODUCTION

Single cantilevered poles, having polygonal or circular cross-sections, can be made of wood, aluminum, steel, reinforced concrete, Fibre Reinforced Polymer (FRP) or combinations of these materials. The main factors that influence the choice of a power supply post are mechanical properties, fabrication, transport and erection expenses, average life and maintenance cost. Permanent load acting on electric poles is from self weight and the weight of electric cables, while the variable load is produced by wind storm, temperature variation and hoar-frost; it has been shown (Kudzys, 2006) that 70% of the electric lines failure have been caused by strong wind and ice storm inducing lateral loading.

Non-prestressed or prestressed steel reinforcement for concrete poles have been successfully used but the corrosion of steel reinforcement has caused high maintenance and replacement cost. The presence of salts, chlorides and other severe aggressive environments such as combination of moisture, temperature variations and sulfate attack are weakening the protection provided by the alkalinity of the concrete on the steel reinforcement thus resulting in corrosion at high rates. Alternatives to deal with this issue have been previously applied using repair techniques of damaged RC poles based on FRP external wrapping (Chahrour and Soudki, 2006). Civil engineers have studied the possibility of mitigating corrosion problems related to steel by replacing it with glass fibre-reinforced polymer composite materials in case of columns (Choo *et al*., 2006) and beams (Almusallam and Al-Salloum, 2006). Introducing of such new advanced composite materials underlined the possibility of avoiding the disadvantages of corrosive, electromagnetic interfering traditional steel reinforcement. Additionally, superior mechanical properties, high strength to weight ratio, revealed the suitability of FRP composite materials for structural uses (Fib Bulletin 40, 2007).

Experimental programs carried out on high strength concrete pylons reinforced with prestressed Carbon Fibre Reinforced Polymeric (CFRP) resins of a 27 m height subjected to bending and to freeze thaw cycles have proven advantages like durability and low self weight by minimizing reinforcement amount and concrete cover (Terrasi *et al*., 2001).

An alternative to enhance the flexural behavior of power transmission hybrid poles is the development of spun cast concrete-filled FRP tubes. Important experimental tests (Naguib and Mirmiran, 2002; Fam and Rizkalla, 2003; Qasrawi and Fam, 2008) and finite element modeling (Fam and Son, 2008) on hybrid concrete-filled

Corresponding Author: Nicolae Taranu, Faculty of Civil Engineering and Building Services, Iasi, 43 Dimitrie Mangeron Blvd., Iasi, 700050, Romania Tel: 40-232-232 219 Fax: 40-232-233 368

FRP tubes with or without steel longitudinal bars have emphasized significant high performance characteristics in bending. Increasing in flexural strength of spun-casting elements utilizing fiber reinforced cementitious composites such as short carbon fibers and polyvinylalcohol (PVA) embedded in a cement matrix has been reported by Kaufmann and Hesselbarth (2007).

The study is focused on the theoretical and experimental analysis of centrifuged concrete poles reinforced with GFRP longitudinal bars and flexible composite spiral reinforcement to avoid the corrosion of steel reinforcing products.

FABRICATION OF THE CENTRIFUGED HYBRID HOLLOW COLUMNS

Generally, the fabrication technology of the centrifuged hybrid hollow concrete columns reinforced with GFRP bars and composite spiral for confinement is based on the one established for columns with steel bars and spirals implemented by Somaco SA, Romania. However, some particularities due to the nature of the materials making up the hybrid product are taken into account and correspondingly treated. The following materials characteristics have been utilized based on the data determined in supplier laboratory (Table 1). GFRP bars for longitudinal reinforcement produced by Fiberline Composites A/S, Denmark and GFPP spiral strip designed by our team and fabricated by CEPROPLAST SRL, Romania. A presentation of the geometric characteristics of all elements is shown in Table 2.

A summary of the technological steps to fabricate the tapered columns follows: the reinforcement cage (Fig. 1) has been set up on rigid fixing rings and this assembly has been placed in the formwork using distance-keepers; six fixing rings have been utilized to set-up the longitudinal reinforcement (8 GFRP bars); the formwork was steel-made (Fig. 2), from two pieces joined by screws; on the formwork length there are transversal circular ribs, guided by the wheels of the centrifuge machine (Fig. 3). The reinforcing cage has been placed in one half of the formwork and then the concrete has been poured; the amount of concrete has been determined so as to fill exactly the formwork; after that, the formwork was closed and placed on the centrifuge machine; a centrifuging time of 15 min, similar to that utilized in case of steel reinforced columns has been selected; about 1 h after the centrifuge operation the formwork has then been kept in place; the formwork has been transported in the treatment chamber and kept for 2 days; the formwork was then removed and the column stored for 28 days until the complete curing of concrete.

Table 1: Summary of mechanical materials properties

Materials	Tensile strength (MPa)	Compressive strength (MPa)	Elastic modulus (GPa)	Ultimate strain (%)
Concrete	-	37.5	36.0	0.35 (compressive)
GFRP bars	1100	-	57.1	0.73 (tensile)
GFPP spiral	225	-	32.0	4.5 (tensile)

Table 2: Summary of geometrical characteristics

Materials	External diameter (mm)	Internal diameter (mm)	Cross sectional dimensions (mm×mm)
Concrete	250	150	-
GFRP bars	16	-	-
GFPP spiral	-	-	11×1.3

Fig. 1: The FRP reinforcement cage

Fig. 2: The steel formwork for centrifuged column

Fig. 3: The rotating wheels of the formwork

THE EXPERIMENTAL PROGRAM

The columns have been tested in horizontal position to bending at an age of 28 days, according to usual procedures, determining the maximum forces and displacement recorded at the free ends of concrete poles reinforced with GFRP bars. Columns with two reinforcing solutions have been fabricated and tested: the first column type specimen with a length of 3 m has been reinforced with smooth GFRP bars and the second type column, 4 m long, has been reinforced with ribbed GFRP bars; the longitudinal profile of both bars are shown in Fig. 4.

An adequate instrumentation has been designed and installed to characterize the structural response of the tested specimens. A specially designed testing stand was constructed to provide the adequate experimental conditions (Fig. 5). The locations of the Linear Voltage Displacement Transducers (LVDTs) to determine the lateral deflections are positioned as shown in Fig. 5. The columns were clamped at one end and the action was exerted by pulling the free end. A loading cell installed on the pulling device has been utilized to measure the corresponding applied load. Successive loading and unloading cycles were applied up to failure and the corresponding displacement for each applied load were measured.

A load-displacement diagram for the 3 m long column reinforced with plain GFRP bars is shown in Fig. 6 for all five loading cycles applied to the specimen. It has been noticed that the first crack occurred at about 4000 N during the third loading cycle; after each cycle the permanent deformation was recorded as shown in Fig. 6. A recorded peak load equal to 6400 N was accompanied by a maximum horizontal displacement equal to 84 mm of the free end. Four meter long specimen has been subjected to eight loading cycles reaching an ultimate peak value equal to 17000 N. In Fig. 7, the repeating load-displacement curves for this specimen are shown. In case of the second column a first crack occurred at 4500 N and a more uniform cracking pattern has been obtained and a maximum horizontal deflection equal to 257 mm has been recorded (Fig. 8). A significant difference have been observed between the behavior of columns reinforced with smooth round GFRP rods and GFRP ribbed rebars, with the geometry visualized in Fig. 4.

Some failure modes typical for the bent cantilevered columns reinforced with GFRP rebars having smooth or ribbed geometries have been observed. Experimental study carried out by other research teams (Hao *et al*., 2007) has revealed the sharp difference between the nature and the values of the bond strength for smooth and ribbed GFRP rebars, explaining the overall behaviour of composite reinforced columns.

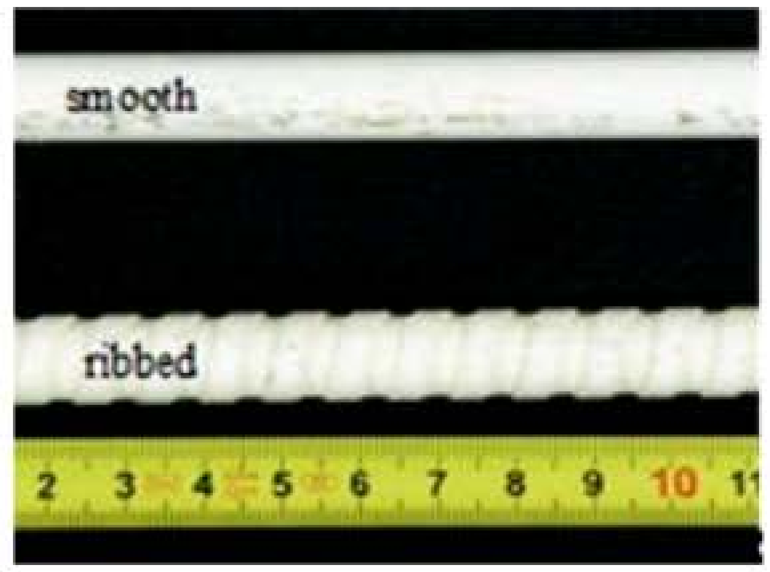

Fig. 4: Types of GFRP longitudinal rebars for the hollow concrete columns

Fig. 5: Instrumentation of the test samples with LVDTs (a) the 3 m long column and (b) the 4 m long column

The cracking process developed progressively, as shown in Fig. 9, until the failure loads have been reached. It has been noticed that the posts failed by concrete crushing, typical for over reinforced elements. The GFRP rebars did not attain their ultimate strength because of the poor bond stress developed between the concrete and the composite bars. A better distribution of cracks (Fig. 9) has been noticed in case of the column reinforced with ribbed bars as a result of better bonding strength between concrete and the GFRP reinforcement. A direct effect of this aspect was the increased failure load (17000 N) and a limited plastic behavior before failure.

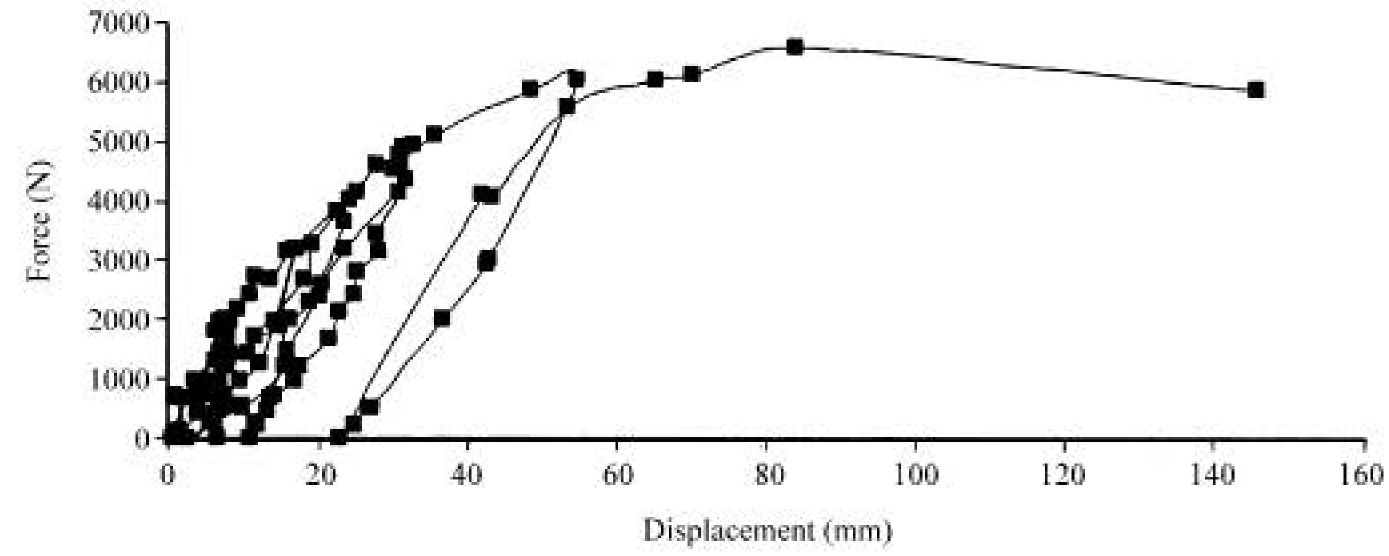

Fig. 6: Force-displacement curve for the 3 m long column corresponding to the end column LVDT (wired transducer 1)

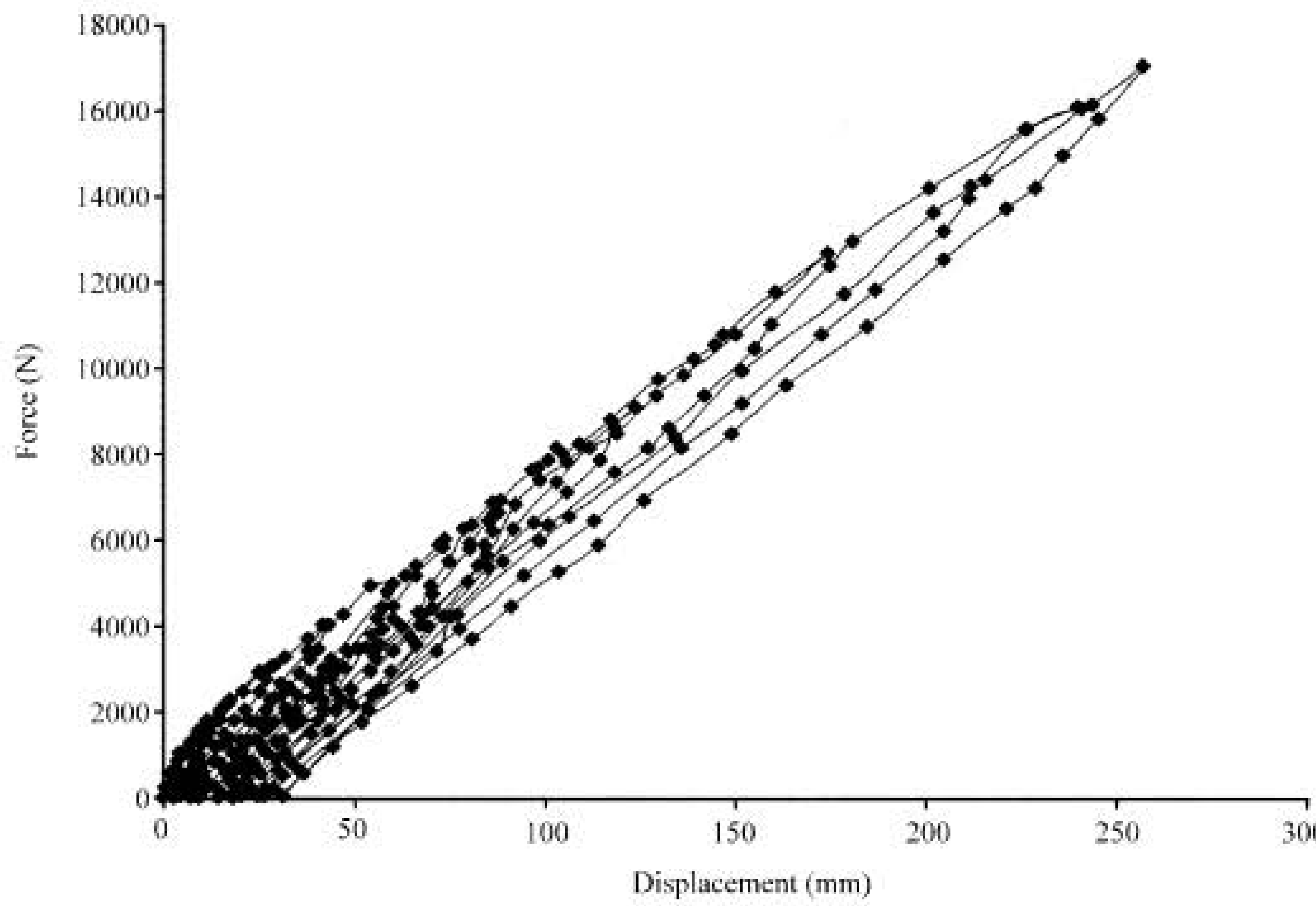

Fig. 7: Force-displacement curves in case of the 4 m long column (wired transducer 0)

Fig. 8: The total displacement at free end of the 4 m specimen

Fig. 9: Crack development in the 4 m long post

Cracks development in the tension part of concrete poles reinforced with GFRP bars due to bending depends on parameters such as crack spacing, bonding strength between composite bars and concrete and strain values in transverse and longitudinal reinforcements (Newhook *et al*., 2002). The spun-cast concrete pole show quite a large displacement at the free end from bending, with ultimate crack observed at around 1.4 m distance from the fixed end of pole, feature that is common in case of experimental pole tests (Kaufmann *et al*., 2005).

THEORETICAL ANALYSIS

Power supply posts are special structural elements whose design although apparently simple raises specific problems. The axial load due to the self weight and power supply installations weight is undertaken exclusively by the concrete area, the FRP considered reinforcement will be subject only to flexural elements design rules, in terms of strength requirements. The determination of bending moment capacity depends on the location of the neutral axis, whose position is determined by equation of equilibrium between the concrete compression and the FRP tension on the cross section. As stated before the post is idealized as a cantilever beam fixed at the bottom end, subjected to flexure caused by the transversely acting loads such as wind pressure or, accidentally, earthquake. Since, the GFRP bars resist only to tensile stress occurring over the cross-section, on the tension side, their contribution in compressive loading resistance is negligible.

In many cases it is considered that the design of such elements is controlled by stiffness, corresponding to serviceability limit state design, by checking the effective deflections versus allowable ones. As far as the ultimate limit state is concerned, there are two accepted failure modes in case of flexural FRP reinforced concrete elements: either concrete crushing or FRP rupture. Both concrete and FRP longitudinal reinforcement are brittle materials determining sudden failure. However, in case of concrete crushing there is a little plastic behavior making this type a slightly more desirable one. Generally, if the design is performed to induce this failure mode, the serviceability requirement concerning the deflections is met.

A particular approach has been used to determine the stiffness of the cantilever column. It has been considered that both concrete and GFRP bars contribute to the total stiffness:

$$K = K_c + K_f \tag{1}$$

where, K is the total bending stiffness of the reinforced column, K_c is the bending stiffness provided by the concrete gross section and K_f is the bending stiffness provided by GFRP bars.

For uniformly tapered poles the moment of inertia of concrete section may be conservatively taken as the gross moment of inertia at a distance one-third of span from the smaller end of the column. The appropriate value of the pole concrete stiffness is also given in the above mentioned report:

$$K_c = \frac{E_c I_g}{2.5} \tag{2}$$

where, E_c is the concrete modulus of elasticity and I_g is the gross moment of inertia of concrete as specified before.

With geometrical and mechanical data already presented $K_c = 8.544\times10^{11}$ N mm^2.

The stiffness provided by the GFRP longitudinal bars has been calculated considering an equivalent composite tubular section having a total area equal to the sum of the cross section of 8 composite bars. Using the characteristics of GFRP bars (Table 1) and the geometry of the reinforcing scheme (Fig. 10), the stiffness value of the composite equivalent tube has been evaluated, $K_f = 5.917\times10^{11}$ N mm^2. Compared the experimental and theoretical elastic deflections determined with total stiffness, K, an approximation of about 7% has been noticed.

Prediction of the most probably way to produce a failure, leading to the ultimate limit state, may be done by comparing the effective FRP reinforcement ratio to the balanced FRP reinforcement ratio. These two parameters are calculated with the following relations:

$$\rho_f = \frac{A_f}{A_g} \tag{3}$$

$$\rho_{fb} = 0.85\beta_1 \frac{f_c'}{f_{fu}} \frac{E_f \varepsilon_{cu}}{E_f \varepsilon_{cu} + f_{fu}} \tag{4}$$

where, ρ_f is the FRP reinforcement ratio, ρ_{fb} is the FRP reinforcement ratio producing balanced conditions, A_f is the GFRP reinforcement area, A_g is the cross-sectional gross area, β_1 is the reduction factor for concrete strength, or stress-block factor for concrete (ISIS Canada, 2001), f'_c is the specified compressive strength of concrete C45/50 (Table 1), f_{fu} is the design tensile strength of GFRP bars, (Table 1), E_f is the guaranteed modulus of elasticity of GFRP, (Table 1) and ε_{cu} is the ultimate strain in concrete, (Table 1).

The ratio of the balanced neutral axis depth c, to the effective depth of the section d_1, can be expressed using strain compatibility shown in Fig. 10:

$$\frac{\varepsilon_{cu}}{c} = \frac{\varepsilon_{frp,1}}{d_1 - c} \tag{5}$$

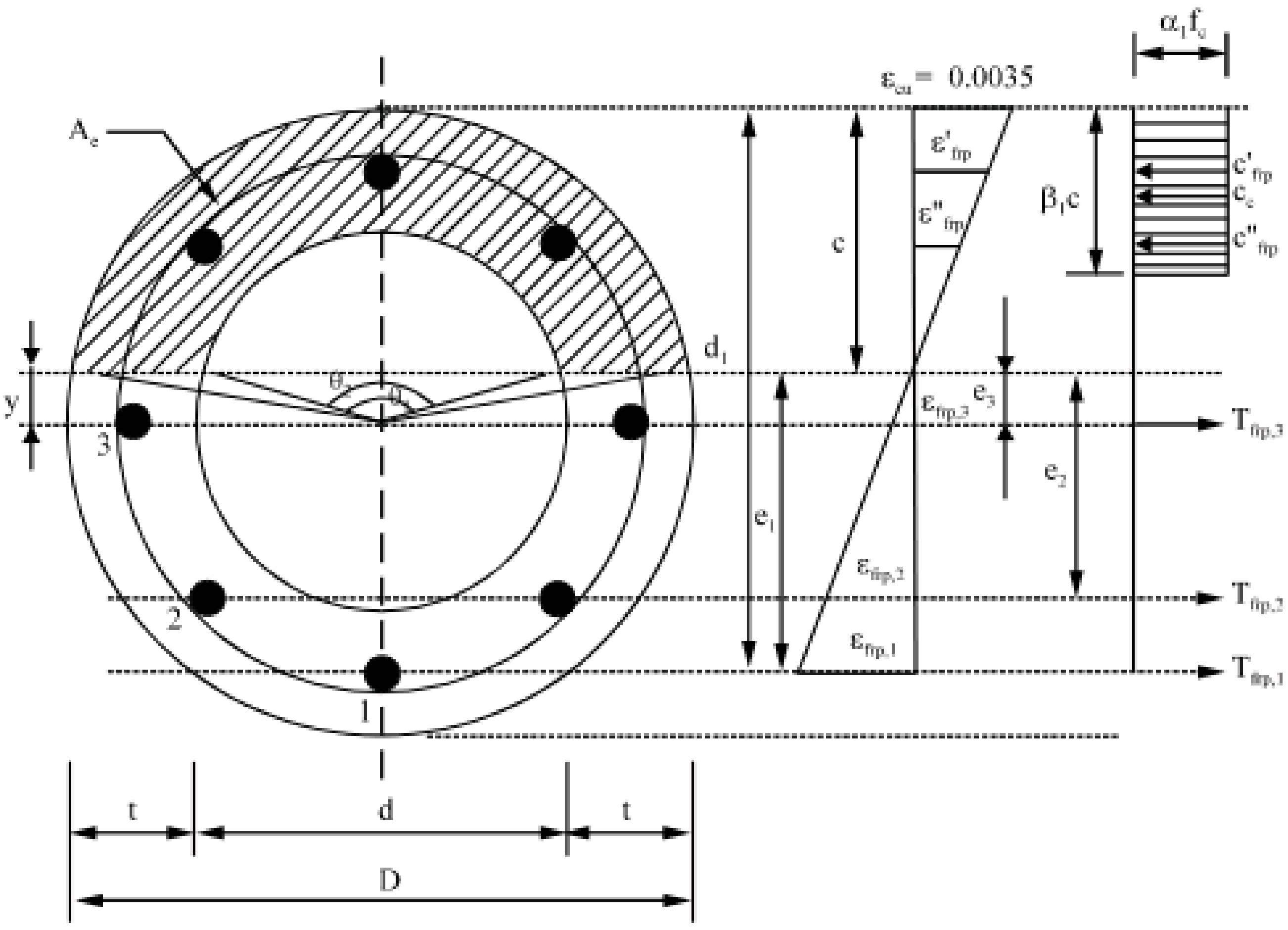

Fig. 10: The reinforcing pattern and the stress-strain distribution in concrete pole reinforced with GFRP

where, ε_{cu} is the ultimate compressive strain in concrete, c is the depth of the neutral axis, d_1 is the effective depth and $\varepsilon_{frp,1}$ is the corresponding value of the strain in FRP.

It has been found by trials that the depth of the neutral axis exceeds the column wall thickness (c = 60 mm). In the next step the compressive and tensile resultants, C_c and T_{frp} are determined. The compression force, C_c, on the concrete section is calculated with:

$$C_c = \alpha_1 \phi_c f_c' \beta_1 A_c \tag{6}$$

where, A_c is the area of the concrete in compression. The coefficients α_1, β_1, ϕ_c are determined according to (ISIS Canada, 2001): α_1 is the stress-block factor for concrete $\alpha_1 = 0.85-0.0015\ f'_c \geq 0.67$, β_1 is the stress-block factor for concrete $\beta_1 = 0.97-0.0025\ f'_c \geq 0.67$ and ϕ_c is the material resistance factor for concrete = 0.65.

The area of concrete in compression A_c shown in Fig. 10, it is equal to the area of the annulus, A_a calculated with (Wang and Salmon, 1979; Kocer and Arora, 1996):

$$A_a = \frac{1}{2}\frac{D^2}{4}(\theta_1 - \sin\theta_1) - \frac{1}{2}\frac{d^2}{4}(\theta_2 - \sin\theta_2) \tag{7}$$

where, D is the external diameter of concrete pole and d is the internal diameter of concrete pole. The values for θ_1, θ_2, the angles figured out in Fig.10, are calculated with:

$$\theta_1 = 2\tan^{-1}\left(\frac{\sqrt{\frac{D^2}{4} - y^2}}{y}\right),\ \theta_2 = 2\tan^{-1}\left(\frac{\sqrt{\frac{d^2}{4} - y^2}}{y}\right) \tag{8}$$

The distance denoted by y, Fig. 10, measured between the neutral axis and the horizontal axis of entire cross section is determined with:

$$y = \frac{Q}{A_a};\ Q = \frac{D^3}{12}\sin^3\left(\frac{1}{2}\theta_1\right) - \frac{d^3}{12}\sin^3\left(\frac{1}{2}\theta_2\right) \tag{9}$$

Using the mechanical and geometrical characteristics of the GFRP reinforced column a value was found for $C_c = 93.85$ kN. The total tensile force T_{frp} of GFRP bars can be expressed as:

$$T_{frp} = \sum_{i=1}^{3} T_{frp,i} = \sum_{i=1}^{3} \phi_{frp} A_{f,i} \varepsilon_{frp,i} E_f \tag{10}$$

where, ϕ_{frp} is the resistance factor for GFRP, 0.4 (ISIS Canada, 2001), $A_{f,i}$ are the areas of the GFRP bars located in the tension region (Fig. 10), $\varepsilon_{frp,i}$ are the strains in the tension GFRP bars (Fig. 10) and i is the current number of GFRP bars (Fig. 10).

After all algebraic calculations, the tensile force was determined: $T_{frp} = 94.69$ kN. These values of C_c and T_{frp} have been evaluated after a number of trials, selecting proper values of c. Since, the column external and internal diameters are known, D = 250 mm and d = 150 mm, the neutral axis depth is also known and the bending moment capacity M_r can been evaluated as:

$$M_r = A_{f,i}\sum_{i=1}^{3} f_{frp,i} e_i + C_c c\left(1 - \frac{\beta_1}{2}\right) \tag{11}$$

where, $f_{rp,i}$ is the tensile stress in the corresponding GFRP bars, denoted 1, 2, 3 in Fig. 10 and e_i represents e_1, e_2, e_3, respectively (Fig. 10).

Table 3: Tensile stress in GFRP bars

Bar No.	Tensile strain	Tensile stress (MPa)
1	0.00962	549.3
2	0.00793	452.8
3	0.00379	216.4

Using the mechanical properties of GFRP bars and corresponding distances, the following effective stress calculated in the reinforcing elements (Table 3).

The bending moment capacity determined with Eq. 11 using the data from Table 3 is M_r = 52.124 k Nm. This value of the column flexural capacity satisfies the condition:

$$M_r \geq 1.5M_{cr} = \frac{f_r I_t}{y_t} \qquad (12)$$

required by ISIS Canada (2001). In Eq. 12 the significance of notations are: M_{cr} is the cracking moment, f_r is the modulus of rupture of concrete equal to $0.6\sqrt{f_c^{'}}$, I_t is the transformed section moment of inertia and y_t is the distance from the neutral axis to the extreme tension fibre.

Using the mechanical and geometrical properties of the GFRP reinforced column, a cracking moment value M_{cr} = 3.206 k Nm has been calculated, that satisfies Eq. 12.

DISCUSSION

Since, the density of steel is 7850 kg m^{-3} and the density of GFRP bars 2200 kg m^{-3}, a saving in weight of about 40% of the reinforcement has been obtained. The result is based on the same number of reinforcing bars utilized for centrifuged hollow columns fabricated with the same technology.

The short term tensile strength of GFRP bars (1100 MPa) is much higher than that of steel bars (435 MPa), but the ultimate long term tensile strength of GFRP bars should be affected by a retention coefficient not exceeding 0.5 for a span life equal to 100 years (Fib Bulletin 40, 2007).

The GFRP bars contribute to the stiffness of the member with 44% less than the steel bar, therefore the total deflection of the hollow column reinforced with composite bars is larger than that reinforced with steel bars.

With a maximum 257 mm lateral deflection, representing a relative displacement equal to 6.67% the column shows a good flexibility under transverse loads.

The two different geometries of the longitudinal GFRP reinforcing bars determine significant differences in structural responses (Fig. 6, 7), in terms of peak force values and lateral displacements. The force-deflection curves underline the superior behavior of the ribbed composite bars hollow column with respect to the smooth bar reinforcing. This superiority can be also noticed in terms of compactness of loading/unloading curves and of residual deformations as well.

CONCLUSION

Hollow concrete columns reinforced with GFRP longitudinal bars and flexible composite spirals can be designed, installed and exploited in a similar manner with the columns reinforced with steel products.

The centrifuged procedure can be utilized to fabricate GFRP reinforced hollow concrete columns. When concrete poles are reinforced with smooth GFRP bars the bonding is not sufficient and this solution does not enable an efficient use of materials characteristics. Ribbed GFRP bars provide a much better bonding enabling the loading of the column to much higher values. Since, the elastic modulus of GFRP bars is only slightly higher then that of concrete, the reinforcement contribution to the stiffness of the element is not substantial. Existing formulas in design norms and codes are suitable for this type of element, having in mind the particularities of composite bars as reinforcements. Finally, all advantages of FRP composite bars (corrosion resistance, lower specific weight, convenient electric and magnetic properties) can be met and valorized in this structural element.

ACKNOWLEDGMENT

This study has been partially supported by a research project on hybrid structures made of polymeric composites and traditional building materials, Program PN II-Idei-Cod 369.

REFERENCES

Almusallam, T.H. and Y.A. Al-Salloum, 2006. Durability of GFRP rebars in concrete beams under sustained loads at severe environments. J. Compos. Mater., 40: 623-637.

Chahrour, A.H. and K.A. Soudki, 2006. Structural retrofitting of deteriorated concrete lighting poles using FRP sheets in wet layup-field application. J. Compos. Const., 10: 234-243.

Choo, C.C., I.E. Harik and H. Gesund, 2006. Strength of rectangular concrete columns reinforced with fiber-reinforced polymer bars. ACI Struct. J., 103: 452-459.

Fam, A. and J.K. Son, 2008. Finite element modeling of hollow and concrete-filled fiber composite tubes in flexure: Optimization of partial filling and design methods for poles. Eng. Struct., 30: 2667-2676.

Fam, A. and S. Rizkalla, 2003. Large scale testing and analysis of hybrid concrete/composite tubes for circular beam-column applications. Const. Build. Mater., 17: 507-516.

Fib Bulletin 40, 2007. FRP Reinforcement in RC Structures. International Federation for Structural Concrete, Sprint-Digital-Druck, Stuttgart.

Hao, Q., Y. Wang, Z. Zang and J. Ou, 2007. Bond strength improvement of GFRP rebars with different rib geometries. J. Zhejiang Univ. Sci. A, 8: 1356-1365.

ISIS Canada, 2001. Design Manual No. 3, Reinforcing Concrete Structures with Fibre Reinforced Polymers. Canadian Network of Centres of Excelence on Intelligent Sensing for Innovative Structures, Winnipeg, Manitoba, ISBN: 0-9689006-6-6.

Kaufmann, J. and D. Hesselbarth, 2007. High performance composites in spun-cast elements. Cement Concrete Compos., 29: 713-722.

Kaufmann, J., D. Hesselbarth, K. Moser and G.P. Terrasi, 2005. Application of fiber reinforced high performance composites in spun-cast elements. Mater. Struct., 38: 549-555.

Kocer, F.Y. and J.S. Arora, 1996. Design of prestressed concrete transmission poles: Optimization approach. J. Struct. Eng. ASCE, 122: 804-814.

Kudzys, A., 2006. Safety of power transmission line structures under wind and ice storms. Eng. Struct., 28: 682-689.

Naguib, W. and A. Mirmiran, 2002. Flexural creep tests and modeling of concrete-filled fiber reinforced polymer tubes. J. Compos. Const. ASCE, 6: 272-279.

Newhook, J., A. Ghali and G. Tadros, 2002. Concrete flexural members reinforced with fiber-reinforced polymer: Design for Cracking and Deformability. Can. J. Civ. Eng., 29: 125-134.

Qasrawi, Y. and A. Fam, 2008. Flexural load tests on new spun-cast concrete-filled fiber-reinforced polymer tubular poles. ACI Struct. J., 105: 750-759.

Terrasi, G.P., G. Battig and R. Bronnimann, 2001. Pylons made of high-strength spun concrete and prestressed with carbon fiber reinforced plastic for high power transmission lines. Proceedings of the ACUN-3 International Composites Conference, Technology Convergence in Composites Application, Feb. 5-9, University of New South Wales, Sydney, Australia, pp: 137-146.

Wang, C. and C.G. Salmon, 1979. Reinforced Concrete Design. 3rd Edn., Harper and Row Publishers, Inc., New York, ISBN: 0700225145.